BIOCHEMISTRY
including biophysical chemistry & molecular biology

Article

pubs.acs.org/biochemistry

# Modifications in Perfringolysin O Domain 4 Alter the Cholesterol Concentration Threshold Required for Binding

Benjamin B. Johnson,[§] Paul C. Moe,[‡] David Wang,[†] Kathleen Rossi,[†] Bernardo L. Trigatti,[†] and Alejandro P. Heuck*[,‡,§]

[†]Department of Biochemistry and Biomedical Sciences, McMaster University, Hamilton, ON, Canada

[‡]Department of Biochemistry and Molecular Biology and [§]Program in Molecular and Cellular Biology, University of Massachusetts, Amherst, Massachusetts 01003, United States

Supporting Information

**ABSTRACT:** Changes in the cholesterol content of cell membranes affect many physiological and pathological events, including the formation of arterial plaques, the entry of virus into cells, and receptor organization. Measuring the trafficking and distribution of cholesterol is essential to understanding how cells regulate sterol levels in membranes. Perfringolysin O (PFO) is a cytolysin secreted by *Clostridium perfringens* that requires cholesterol in the target membrane for binding. The specificity of PFO for high levels of cholesterol makes the toxin an attractive tool for studying the distribution and trafficking of cholesterol in cells. However, the use of the native toxin is limited given that binding is triggered only above a determined cholesterol concentration. To this end, we have identified mutations in PFO that altered the threshold for how much cholesterol is required to trigger binding. The cholesterol threshold among different PFO derivatives varied up to 10 mol % sterol, and these variations were not dependent on the lipid composition of the membrane. We characterized the binding of these PFO derivatives on murine macrophage-like cells whose cholesterol content was reduced or augmented. Our findings revealed that engineered PFO derivatives differentially associated with these cells in response to changes in cholesterol levels in the plasma membrane.

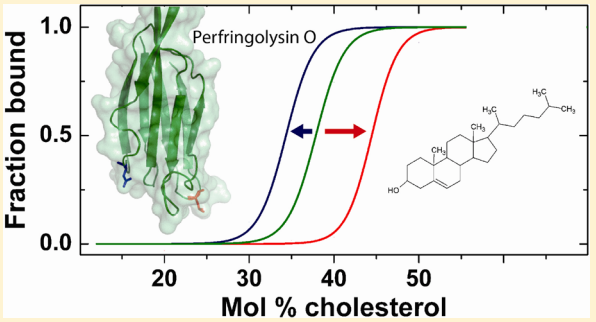


Cholesterol is an essential component of mammalian cell membranes, and its distribution on cell membranes is tightly regulated.[1,2] In mammalian cells, this sterol is derived either from low-density lipoprotein (LDL) receptor-mediated endocytosis and subsequent hydrolysis in lysosomes or via de novo biosynthesis in the endoplasmic reticulum.[3] The mechanism of intracellular cholesterol transport and distribution is an unresolved issue of fundamental importance to cell biology and medicine.[4] Defects in these transport pathways can alter the cellular cholesterol metabolism, resulting in pathological states.[5] Abnormal cholesterol levels have been implicated in several diseases, including atherosclerosis,[6,7] Niemman-Pick type C disease,[8,9] and Alzheimer's disease,[10] among others. Understanding the pathways of intracellular cholesterol transport constitutes a critical step toward the adjustment of abnormal cholesterol levels in mammalian cells and many other cellular cholesterol lipidoses.[11,12]

Among the most powerful tools for assessing the localization and fluctuations of molecules, in the physiological context of intact living cells, are fluorescence microscopy and related techniques. Given the remarkable improvements in fluorescence imaging technology,[13,14] visualization of cholesterol molecules in membranes is limited only by the molecular probes available to directly determine cholesterol levels.[15,16] Cholesterol-binding reagents like filipin, a fluorescent polyene antibiotic, have been widely used to stain cholesterol in cell membranes.[17,18] However, given the ubiquitous distribution of cholesterol in mammalian cells, membrane permeable filipin and other cholesterol fluorescent analogues commonly employed as imaging probes[12,16] stain all membranes (i.e., plasma and inner membranes).[9] Clearly, better molecular probes could facilitate the detection of cholesterol levels in cell membranes and their fluctuation in response to metabolic signals and drug therapies.

Nonlytic derivatives of the cholesterol-dependent cytolysin (CDC) perfringolysin O (PFO) have been used to detect cholesterol rich microdomains in cell membranes.[19] PFO is secreted as a water-soluble protein that upon binding to a cholesterol-containing membrane, oligomerizes and spontaneously inserts into the bilayer to form a large $\beta$-barrel pore (diameter of ~300 Å).[20] In contrast to filipin, which binds indiscriminately to cholesterol in membranes,[18,21] it has been shown that PFO binds to membranes only when the cholesterol concentration exceeds a certain threshold.[22,23] The sharp transition observed for binding of PFO to model membranes containing increasing amounts of cholesterol

**Received:** March 5, 2012
**Revised:** April 6, 2012
**Published:** April 6, 2012

  

suggests that the toxin could be used as a molecular probe to detect cholesterol levels on cell membranes. Unfortunately, the promise of PFO as a cholesterol imaging probe is limited by the narrow spectra of cholesterol concentrations that can be discriminated by the native toxin. It has been also suggested that PFO binds to cholesterol rich membranes or membrane rafts.[24,25] However, it has become clear that exposure of cholesterol and concomitant PFO binding depends on the overall composition of the membrane.[26−29] The head size or the presence of unsaturated acyl chains on the phospholipids forming the membrane can alter the amount of cholesterol required to trigger binding.

Binding of PFO to cholesterol is sufficient to trigger all the conformational changes required to form an oligomer,[30] and the C-terminus of PFO or domain 4 (D4) guides the first contact of the toxin with the membrane.[23] Toxin−membrane interaction occurs via the distal loops that connect the eight $\beta$-strands that form the D4 $\beta$-sandwich. Three of these loops are highly conserved among the CDC members, and in addition to the conserved undecapeptide loop (amino acids 458−468), it has been shown that two residues located in loop 1 (L1), Thr490 and Leu491, are essential for the recognition of cholesterol at the membrane surface.[31,32]

We have recently found that the Cys459Ala modification of the membrane interacting domain of PFO D4 alters the cholesterol concentration threshold required for binding.[28] We reasoned that additional modifications may yield PFO derivatives that bind to membranes containing more or less cholesterol than the native toxin. By combining the tunable properties of PFO D4 with the many fluorescent probes available,[15] we are able to generate imaging reagents capable of detecting a broad range of distinct cholesterol levels in cell membranes.

These studies revealed that modifications of residues located in the proximity of Cys459 raised or lowered the cholesterol concentration threshold for PFO binding. Therefore, using a lytic-impaired parental PFO derivative,[33,34] we generated mutants that bound to higher or lower cholesterol concentrations in model membranes. Replacement of the charged Asp434 residue with Ser lowered the cholesterol threshold of the parental PFO, while replacement of the nonpolar Leu491 with Ser increased the amount of cholesterol required in the membrane to trigger binding. When tested with model membranes, the threshold required to trigger binding for these PFO derivatives expanded more than 10 mol % cholesterol. The differential binding properties of the generated PFO derivatives did not vary with changes in the membrane composition, and more importantly, these properties were also observed when the PFO derivatives were used on native murine macrophage-like cell membranes.

## EXPERIMENTAL PROCEDURES

**Preparation of PFO Derivatives.** The expression and purification of the PFO derivatives were conducted as described previously.[27,30,35] The PFO derivative containing the native sequence (amino acids 29−500) and the polyhistidine tag that came from the pRSETB vector (Invitrogen) is named nPFO.[27] The PFO Cys-less derivative ($nPFO^{C459A}$, where Cys459 is replaced with Ala) is named rPFO.[35] The single-Cys lysis-impaired parental derivative used in this study ($rPFO^{E167C/F318A}$) was named $_{F}$PFO. The E167C mutation on domain 1 (D1) provides a site for specific probe attachment,[34] and the F318A mutations on D3 eliminate the lytic activity of the toxin on liposomes.[33] Mutagenesis of PFO was done using the QuickChange (Stratagene) procedure as described previously.[36]

**Steady-State Fluorescence Spectroscopy.** Steady-state fluorescence measurements were taken using a Fluorolog-3 photon-counting spectrofluorometer as described previously.[28] Samples were equilibrated at 25 °C before fluorescence was determined.

**Assay for Binding.** Binding to liposomes was done using the change in the Trp emission intensity produced by the binding of PFO to cholesterol-containing membranes as described previously.[28] Briefly, emission for Trp fluorescence was recorded at 348 nm (4 nm bandpass) with the excitation wavelength fixed at 295 nm (2 nm bandpass). The signals of monomeric PFO derivatives were obtained with samples containing 200 nM protein in buffer A [50 mM HEPES, 100 mM NaCl, 1 mM DTT, and 0.5 mM EDTA (pH 7.5)] using 4 mm × 4 mm quartz cuvettes.[37] The net emission intensity ($F_0$) for monomers was obtained after subtracting the signal of the sample before the protein was added. Liposomes were added (~200 $\mu$M total lipids), and the samples were incubated for 20 min at 37 °C. Trp emission after membrane incubation was measured after re-equilibration of the sample at 25 °C, and the signal from an equivalent sample lacking the protein was subtracted ($F$). The fraction of protein bound was determined as $(F - F_0)/(F_f - F_0)$, where $F_f$ is the emission intensity when all the protein is bound. Binding of PFO derivatives to cholesterol dispersions in aqueous solutions was conducted as described previously.[30]

**Urea Unfolding Equilibrium Studies.** Unfolding was conducted as described previously.[28] The conformational stability of the proteins ($\Delta G_{U-F}^{water}$) was calculated assuming a two-state unfolding model for the PFO monomers.

**Labeling of the Fluorescent Protein.** Fluorescent labeling was conducted as previously described.[34,38] Maleimide derivatives of Alexa 488 or 633 were mixed with the PFO derivative of interest and incubated at room temperature for 2 h in buffer B [50 mM HEPES and 100 mM NaCl (pH 8)]. Labeled PFO was separated from the free dye by size exclusion chromatography using Sephadex G-25 [1.5 cm (inside diameter) × 25 cm column].

**Preparation of Lipids and Liposomes.** Nonsterol lipids were obtained from Avanti Polar Lipids (Alabaster, AL), and cholesterol was from Steraloids (Newport, RI). Large unilamellar vesicles were generated as described previously.[39] Briefly, equimolar mixtures of 1-palmitoyl-2-oleoyl-*sn*-glycero-3-phosphocholine (POPC), 1-palmitoyl-2-oleoyl-*sn*-glycero-3-phosphoethanolamine (POPE), and sphingomyelin (SM, porcine brain) were combined with the indicated amount of cholesterol (5-cholesten-3$\beta$-ol) in chloroform. The thin film of lipids formed after chloroform evaporation was resuspended in buffer A and passed through an extruder equipped with a 0.1 $\mu$m filter 21 times. Liposomes were stored on ice and discarded after 3 weeks.

**Lipid Determination.** The percentage of cholesterol in liposomes used in Figure 3A was determined using the Amplex Red Cholesterol Assay Kit (Invitrogen). The total phosphate quantification assay was as described by Chen et al.[40] Briefly, the lipid samples (30 $\mu$L) were added to a mixture of 0.45 mL of 8.9 M sulfuric acid and 0.15 mL of hydrogen peroxide (30%, v/v) and heated at 200−215 °C for 30 min. The sample was then allowed to cool for 5 min at 20−23 °C, and 3.9 mL of water, 0.5 mL of 20 mM ammonium molybdate, and 0.5 mL of

0.57 M ascorbic acid were added and mixed after each addition. Samples were then heated at 100 °C for 5 min, and the absorbance at 800 nm was determined after equilibration at 25 °C. Readings were then compared to a standard curve obtained in parallel with samples of potassium phosphate of known concentrations to determine the concentration of individual samples. The mole percent of cholesterol in each sample was calculated as total cholesterol/(total phosphate + total cholesterol). For other experiments, the concentration of lipids was calculated using the concentration of stock solutions (usually within ±3% of measured concentrations).

**Preparation of Cyclodextrin Complexed with Cholesterol.** Methyl-β-cyclodextrin (mβCD) and cholesterol were from Sigma-Aldrich Canada Ltd. (Oakville, ON). mβCD−cholesterol complexes were prepared as described by Christian et al.[41] Briefly, cholesterol dissolved in a chloroform/methanol mixture (1:1 by volume) was transferred to a glass tube, and the solvent was evaporated under $N_2$ gas passed through a 0.2 μm syringe filter. mβCD (2.5 mM in Dulbecco's modified Eagle's medium) was added to the cholesterol residue to the desired mβCD:cholesterol molar ratio. Cholesterol was dissolved by sonication for 30 min in a bath sonicator, followed by the sample being mixed overnight at 37 °C. Samples were sterilized by being passed through 0.45 μm syringe filters and used immediately thereafter. All procedures were performed in glass.

**Cell Culture.** All reagents for cell culture were from Life Technologies Inc. (Burlington, ON). RAW 264.7 murine macrophage-like cells were cultured in Dulbecco's modified Eagle's medium containing 10% fetal bovine serum (heat-inactivated), 2 mM L-glutamine, 50 units/mL penicillin, and 50 μg/mL streptomycin. Cells were passaged when they reached 75% confluence by being gently scraped and plated at a 1:5 ratio in fresh medium. Prior to each experiment, $3 \times 10^5$ cells were seeded into each well of an eight-well Nunc LabTek Chambered Coverglass (Thermo Scientific) and cultured for 24 h.

**Treatment of Cells, Labeling, and Fluorescence Microscopy.** Cells were treated for 1−3 h at 37 °C with medium containing either filipin (5 μg/mL; Sigma-Aldrich Canada Ltd.), mβCD (at the concentrations indicated), 2.5 mM mβCD complexed to cholesterol at different mβCD:cholesterol ratios, or no additions. Cells were then washed twice with cPBS [0.88 mM $KH_2PO_4$, 6.4 mM $Na_2HPO_4$, 136.8 mM NaCl, and 2.7 mM KCl (pH 7.4) (PBS) supplemented with 1 mM $CaCl_2$], fixed for 30 min at 23−25 °C with 2.5% paraformaldehyde (freshly made in PBS), and washed twice with PBS. Cells were incubated with fluorescently labeled PFO derivatives (38 nM in PBS containing 1 mg/mL bovine serum albumin) as indicated, for 90 min at 37 °C. In some experiments, cholera toxin subunit B (CTxB) labeled with Alexa 594 [5 μg/mL (Life Technologies Inc.)] was included in the incubation. Cells were then washed once with PBS at 23−25 °C, and for some experiments, cells were stained with DAPI [4′,6-diamidino-2-phenylindole, 300 nM, 1 min in PBS at 20−23 °C (Life Technologies Inc.)]. Cells were washed another three times with PBS at 23−25 °C, and cPBS containing 0.5 mM ascorbic acid (Sigma Chemical Co., St Louis, MO) was added. Cells were immediately imaged by wide-field fluorescence microscopy using either a Zeiss Axiovert 200 M or a Leica DMI 6000B fluorescence microscope.

## RESULTS

**The Amount of Cholesterol Required To Trigger Binding of PFO to a Membrane Is Affected by Amino Acids Located around the Conserved Cys459.** The binding of PFO to model membranes is regulated by both the lipid composition of the membrane and the structure of the loops located at the distal tip of D4 (Figure 1A). The presence

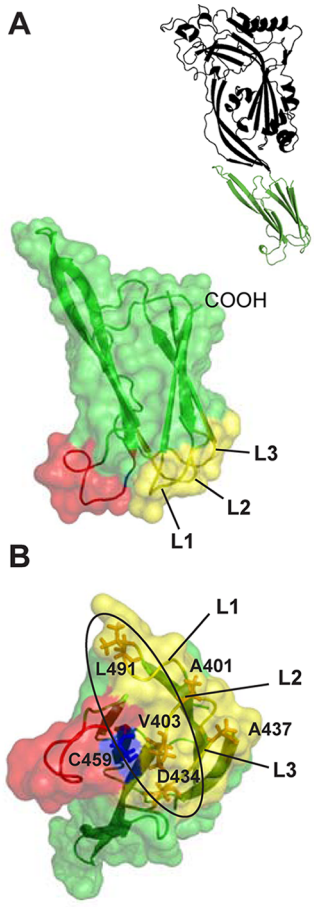


**Figure 1.** PFO D4 showing the location of residues modified in this study. (A) Cartoon representation of the α-carbon backbone for PFO (top right) with D4 colored green and for the α-carbon backbone and amino acids surface side view of PFO D4. The conserved undecapeptide (red), C459 (blue), the three loops (L1−L3) located at the tip of D4 (yellow), and the C-terminus are indicated. (B) Bottom view of the cartoon representation shown in panel A, with amino acids mentioned in the text shown as sticks and labeled. The central region containing mutations that affect the cholesterol threshold of the toxin is surrounded by an oval. The image of PFO D4 was rendered in PyMol (DeLano Scientific).

of "free" cholesterol molecules at the membrane surface is required to trigger PFO−membrane association.[20,27,28,30] However, how many of these free cholesterol molecules are required to trigger binding seems to be dictated by the structure of the D4 loops. Using POPC/cholesterol liposomes as model membranes, we have recently shown that the Cys459 to Ala substitution raised the threshold for cholesterol binding from 30 to 35 mol %.[28] This was surprising because it has been shown that only loop 1 (L1), loop 2 (L2), and loop 3 (L3) in D4 mediate the specific interaction of PFO with cholesterol,[32] with only two residues (Thr490 and Leu491) being essential


dx.doi.org/10.1021/bi3003132 | Biochemistry 2012, 51, 3373−3382

for cholesterol recognition.[31] It is clear from these data that the precise role of cholesterol in the cooperative cytolytic mechanism of PFO is far from being understood.

We therefore investigated first if the phospholipid composition of the membrane affected the differential binding of native nPFO and the Cys-less rPFO and second if modifications to residues that are known to interact with the membrane upon PFO binding further affected the cholesterol binding threshold of the toxin.[35] The cholesterol content of the liposomes was varied from 25 to 50 mol %, and the phospholipid composition was fixed at a 1:1:1 POPC:POPE:SM molar ratio (the most abundant human plasma membrane phospholipids). In membranes containing just POPC and cholesterol, the cholesterol thresholds for nPFO and rPFO binding are 40 and 44 mol % cholesterol, respectively.[28] In membranes containing POPC, POPE, and SM, the cholesterol thresholds for nPFO and rPFO binding were 36.5 and 41.5 mol % cholesterol, respectively. Interestingly, despite the fact that both PFO derivatives showed a lower cholesterol threshold when a more complex phospholipid mixture was used, the cholesterol mole percent difference between the PFO derivatives remained constant (Figure 2A).

Four mutants of the Cys-less rPFO derivative, L491C (in L1), A401C and V403C (in L2), and A437C (in L3) (Figure 1),[35] were initially tested to evaluate the effect of D4 mutations on the cholesterol-dependent binding of PFO. The pore forming activity of these derivatives is similar to that of nPFO when measured using liposomes containing a high level of cholesterol.[35] Two of the analyzed mutants, rPFO$^{L491C}$ and rPFO$^{V403C}$, showed a 4−5 mol % increase in the cholesterol concentration required to trigger binding (Figure 2A). No major change was observed for the A437C mutant and a minimal change for the A401C substitution. A close inspection of the structure of the D4 distal tip shows that the Leu491 and Val403 residues are proximal to Cys459 (Figure 1B), while A401 and A437 are more distant from the undecapeptide. To evaluate the potential effect of D4 mutations on the conformational stability of the protein, we determined the free energy for the unfolding of rPFO$^{L491C}$, the protein with the highest cholesterol threshold, using equilibrium urea denaturation (Figure 2B).[28] No significant difference in $\Delta G_{U-F}{}^{water}$ was observed between rPFO and rPFO$^{L491C}$ (13.6 ± 1.5[28] and 13.2 ± 1.6 kcal/mol, respectively). These results suggest that mutations that altered the cholesterol threshold of rPFO did not affect the stability of the toxin. Moreover, nPFO and rPFO$^{L491C}$ bound similarly to cholesterol dispersed in aqueous buffer (Figure 2C),[30] suggesting that the change in the cholesterol threshold is not related to the ability of the proteins to bind cholesterol. The lower maximal $F/F_0$ observed for rPFO$^{L491C}$ is typical for PFO derivatives containing the Cys459 to Ala mutation, which have higher $F_0$ values.[28]

**A Standard Scale for Evaluating the Binding Properties of PFO Mutants.** The changes in the intrinsic Trp fluorescence that follows membrane binding of PFO derivative have been effectively used to determined the fraction of protein bound as a function of cholesterol concentration.[23,27−30] The steplike increase in Trp emission intensity for PFO derivatives occurred at a precise cholesterol concentration (Figure 2A). Each PFO derivative is therefore characterized by a cholesterol threshold defined as the cholesterol concentration at which the increase in Trp emission is half of the emission when binding is complete. Because the absolute cholesterol threshold (mole percent) depends on the lipid composition of the membranes (see above) and there are small variations in the cholesterol concentration among identically prepared liposome batches (~5 mol % in our hands), it is convenient to define a relative value for the cholesterol threshold rather than an "absolute" value. The difference in the cholesterol threshold (change in the mole percent of cholesterol obtained with the same membranes) between nPFO and the PFO mutant under study is a more robust parameter for characterizing the cholesterol binding properties of PFO derivatives. A negative value of the change in the mole percent of cholesterol indicates a derivative that binds at lower cholesterol concentrations than nPFO, and

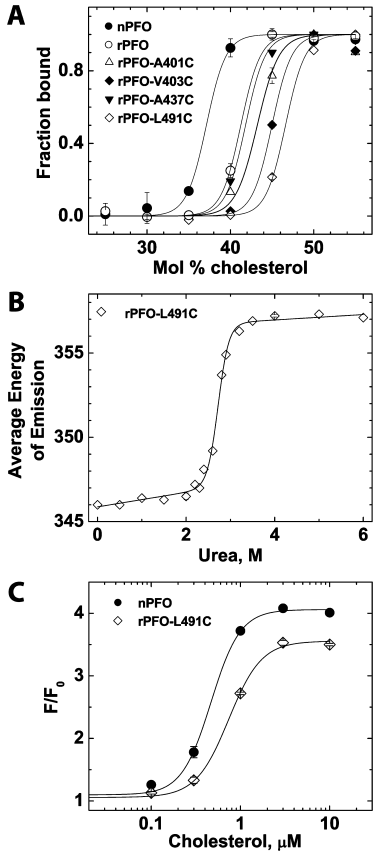


**Figure 2.** Mutations on D4 alter the cholesterol threshold of PFO. (A) The fraction of bound PFO derivatives (final concentration of 0.1 $\mu$M) to liposomes of varying cholesterol content and POPC, POPE, and SM in a constant 1:1:1 ratio (final total lipid concentration of 0.1 mM) was determined using intrinsic Trp fluorescence as described in Experimental Procedures. The cholesterol thresholds for both nPFO and rPFO were lower than those observed with POPC and cholesterol,[28] but the difference in the cholesterol threshold (~5 mol % cholesterol) was not significantly affected by the change in the phospholipid composition of the membrane. A >4 mol % increase in the cholesterol threshold was observed for the rPFO$^{V403C}$ and rPFO$^{L491C}$ mutants. (B) Urea denaturation for rPFO$^{L491C}$, the derivative with the highest cholesterol threshold. The average energy of emission for each fluorescence emission spectrum was obtained at given urea concentrations. The data were fit assuming that the average energy of emission of the folded and unfolded states varies linearly with urea concentration. (C) Binding of nPFO (●) and rPFO$^{L491C}$ (◇) to cholesterol dispersed in an aqueous buffer solution. The Trp emission intensity for 0.1 $\mu$M protein was measured as described in Experimental Procedures before ($F_0$) or after ($F$) addition of the indicated amount of cholesterol. Most data points show the average of at least two independent measurements and their range.


dx.doi.org/10.1021/bi3003132 | *Biochemistry* 2012, 51, 3373−3382

a positive value indicates that higher cholesterol concentrations are required for binding. For example, we found previously that rPFO required more cholesterol than nPFO for membrane binding.[28] Using the relative scale defined above, the corresponding change in the mole percent of cholesterol for rPFO is +3.6. The absolute cholesterol threshold value for any PFO derivative can be calculated using the values of the change in the mole percent of cholesterol if the value for nPFO is known for a particular membrane system. We therefore determined the cholesterol threshold for nPFO by quantification of the lipid composition of liposomes with a 1:1:1 POPC:POPE:SM molar ratio and various amounts of cholesterol (Figure 3A). The cholesterol threshold of nPFO was 36.5 ± 1 mol % cholesterol for this membrane system.

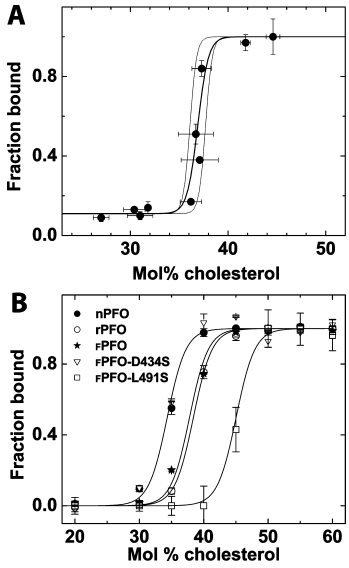


**Figure 3.** Cholesterol thresholds in PFO derivatives can differ by up to 10 mol % cholesterol. (A) Determination of the cholesterol threshold for nPFO (final concentration of 200 nM) on POPC/POPE/SM membranes containing the indicated mole percent of cholesterol (final total lipid concentration of 100 $\mu$M). The mole percent of cholesterol was determined by individual quantification of cholesterol and total phospholipids. Cholesterol was quantified using Amplex Red, and total phospholipids were quantified by phosphate determination after acid hydrolysis as described in Experimental Procedures. Thin lines are a guide for the eye to indicate the average range for data in the transition. (B) Cholesterol-dependent binding of $_{F}$PFO$^{D434S}$ (▽) and $_{F}$PFO$^{L491S}$ (□) derivatives selected for cellular studies compared to nPFO (●), rPFO (○), and $_{F}$PFO (★). Binding measurements were taken as described in the legend of Figure 2. Data points are the average of at least two measurements and their standard deviation.

**Mutations on D4 Can Increase or Decrease the Change in the Mole Percent of Cholesterol of PFO Derivatives.** Our ultimate goal is to obtain probes that differentially bind to cellular membranes containing different levels of cholesterol. We therefore introduced single-amino acid mutations into PFO D4 using the parental rPFO$^{E167C/F318A}$ derivative (hereafter named $_{F}$PFO). The F318A mutation renders a protein that oligomerizes on liposomal membranes but is not lytic at a 1:1000 protein:total lipid concentration ratio[33] and increases by >20-fold the magnitude the toxin dose required to cause 50% hemolysis in sheep red blood cells (see the Supporting Information). The E167C mutation introduces a unique site for labeling with a fluorescent or other probe of choice, and this modification does not affect the properties of the toxin.[30,34] We first evaluated the cholesterol threshold for the parental $_{F}$PFO derivative, which contains the same D4 as rPFO. The change in the mole percent of cholesterol for $_{F}$PFO was +3.2 ± 0.5, very similar to that observed for rPFO (Figure 3B). This result clearly indicated that neither the F318A mutation in D3 nor the E167C mutation in D1 affected the cholesterol binding properties of the toxin. Our next goal was to scan the D4 loops for mutations that raised or lowered the cholesterol threshold of $_{F}$PFO.

Our first candidate for decreasing the cholesterol threshold was the charged D434 residue located in L3 of PFO D4. The negatively charged Asp was modified to Ser, a noncharged amino acid that can form hydrogen bonds with the polar groups of the lipids at the membrane surface. The change in the mole percent of cholesterol for $_{F}$PFO$^{D434S}$ decreased ~3 units, rendering a derivative with a cholesterol threshold lower than that of the parental $_{F}$PFO derivative and very similar to that for nPFO (Figure 3B).

With the goal of raising the cholesterol threshold of the $_{F}$PFO derivative to higher cholesterol concentrations, we targeted the L491 residue because it has been shown that the L491A mutation weakened PFO binding as determined using surface plasmon resonance.[31] We replaced the hydrophobic Leu with the more polar Ser, generating the $_{F}$PFO$^{L491S}$ derivative. As expected, $_{F}$PFO$^{L491S}$ showed a cholesterol threshold 7 units higher than that of the parental $_{F}$PFO (Figure 3B). Both $_{F}$PFO$^{D434S}$ and $_{F}$PFO$^{L491S}$ were selected for cellular studies because the cholesterol threshold between them differs by more than 10 mol % cholesterol.

**Cholesterol Was Essential for Binding of PFO to Murine Macrophage-like Cells.** We tested if the binding of the parental $_{F}$PFO$^{Alexa488}$ derivative was dependent on cholesterol at the surface of the plasma membrane of murine macrophage-like cells using two independent assays. First, we incubated murine macrophage-like cells with the cholesterol binding polyene filipin to block cholesterol at the membrane surface.[42−44] While filipin fluorescence was seen at the cell surface and intracellularly (Figure 4A), $_{F}$PFO$^{Alexa488}$ was found only at the surface of untreated murine macrophage-like cells. In contrast, when cells were first treated with filipin, no significant binding of $_{F}$PFO$^{Alexa488}$ was detected on the cell surface (Figure 4A). Cholera toxin subunit B associates with lipid rafts in plasma membranes by binding to ganglioside GM1 in a cholesterol-independent manner.[45] Labeling of cells with CTxB$^{Alexa594}$ was not affected by filipin treatment, demonstrating that filipin treatment did not disrupt the plasma membrane but specifically blocked $_{F}$PFO$^{Alexa488}$ binding. Second, we tested the cholesterol dependence of binding of $_{F}$PFO$^{Alexa488}$ to murine macrophage-like cells by removing cholesterol from the membrane surface using incubation with m$\beta$CD.[46] Cells were incubated with 0.05, 0.5, or 5 mM m$\beta$CD for 3 h at 37 °C. Treatment of cells with ≥0.5 mM m$\beta$CD prevented labeling with $_{F}$PFO$^{Alexa488}$, whereas treatment with ≤0.05 mM m$\beta$CD (Figure 4B) (data not shown) had no apparent effect . In contrast, treatment of cells of m$\beta$CD did not affect the extent of CTxB$^{Alexa594}$ binding. It is clear from these data that binding of $_{F}$PFO$^{Alexa488}$ to plasma membranes of murine macrophage-like cells was dependent on the presence of cholesterol and regulated by the cholesterol levels at the membrane surface.

**The Sensitivity of PFO Mutants to Cholesterol Concentration Was Conserved on Murine Macrophage-like Cell Membranes.** The cholesterol content of

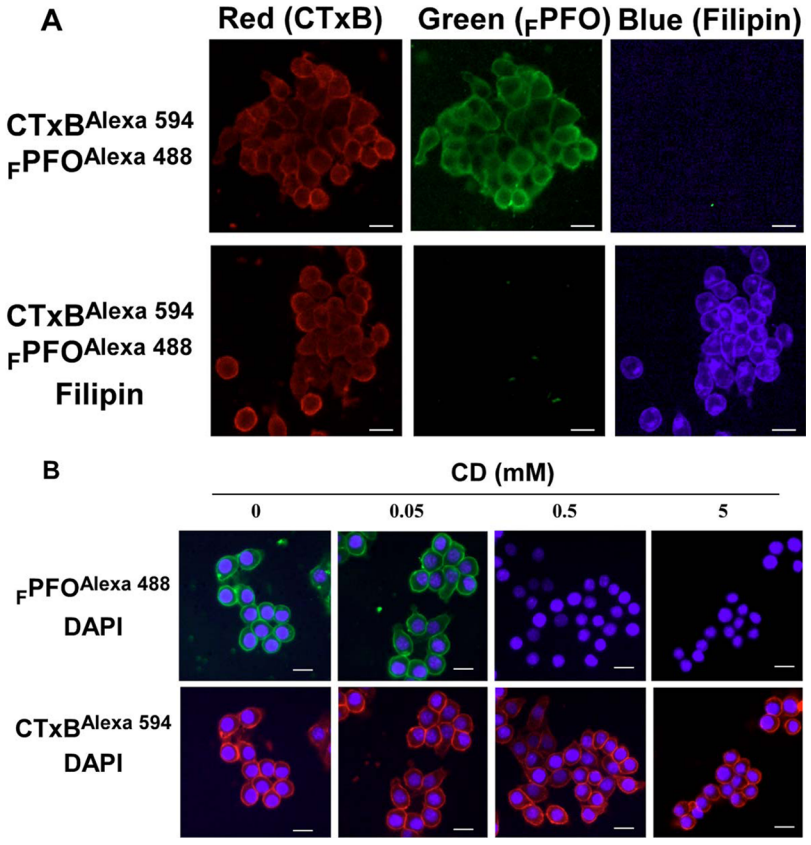


**Figure 4.** Cholesterol modulates binding of $_F$PFO to murine macrophage-like cells. (A) Filipin blocks binding of $_F$PFO$^{Alexa488}$ to the cell surface. Fixed RAW 264.7 murine macrophage-like cells were incubated without (top) or with 7.6 $\mu$M filipin (bottom) for 60 min at 20−23 °C. Cells were washed and incubated with $_F$PFO$^{Alexa488}$ (40 nM) and CTxB$^{Alexa594}$ (5 $\mu$g/mL) (the latter as a marker for the cell surface). (B) Depletion of cholesterol using m$\beta$CD inhibits $_F$PFO$^{Alexa488}$ binding. Cells were treated for 2 h without (panels marked 0) or with the indicated amount of m$\beta$CD. Cells were then fixed and incubated with $_F$PFO$^{Alexa488}$ and CTxB$^{Alexa594}$ for 90 min and then stained with DAPI for nuclear DNA as described in Experimental Procedures. Labeled cells were imaged by wide field fluorescence microscopy using standard filter sets for TRITC ("Red" CTxB labeling), FITC ("Green", $_F$PFO$^{488Alexa}$), or DAPI ("Blue", filipin labeling in panel A and DAPI labeling in panel B). Scale bars represent 10 $\mu$m.

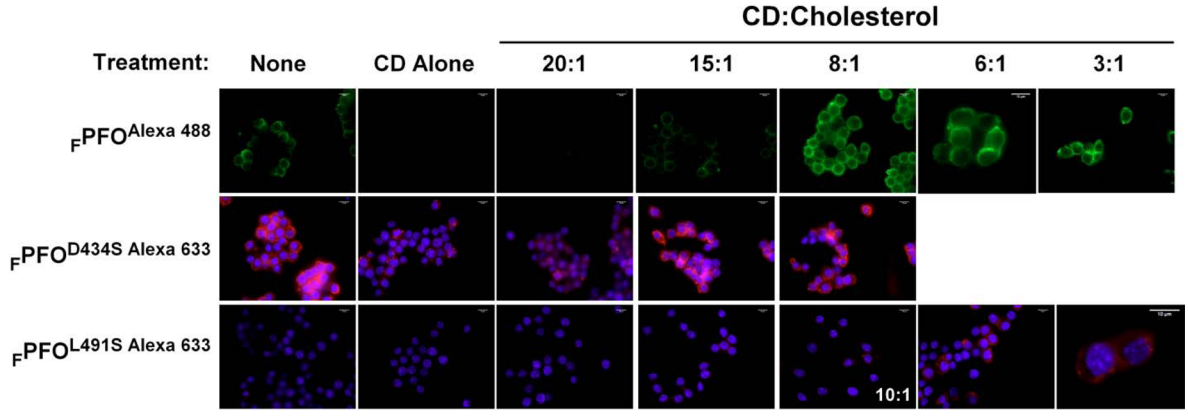


**Figure 5.** Different cholesterol levels are distinguished by PFO derivatives on murine macrophage-like cell membranes. RAW 264.7 cells were incubated for 3 h at 37 °C either with no additions (panels marked None), with 2.5 mM m$\beta$CD alone, or with 2.5 mM m$\beta$CD complexed with cholesterol at the indicated m$\beta$CD:cholesterol ratios. After 3 h, cells were washed, fixed, and incubated with 38 nM $_F$PFO$^{Alexa488}$ (top), $_F$PFO$^{D434S\ Alexa633}$ (middle), or $_F$PFO$^{L491S\ Alexa633}$ (bottom). Cells labeled with $_F$PFO$^{D434S\ Alexa633}$ or $_F$PFO$^{L491S\ Alexa633}$ were also incubated with DAPI (middle and bottom). Cells treated with m$\beta$CD:cholesterol ratios of 6:1 and 3:1 were not incubated with $_F$PFO$^{D434S\ Alexa633}$ (middle). Scale bars represent 10 $\mu$m.

the cell membranes can be altered by incubations with m$\beta$CD or mixtures of m$\beta$CD and cholesterol.[46] Incubations with m$\beta$CD alone or with high m$\beta$CD:cholesterol ratios reduce the cholesterol concentration on the plasma membrane. In contrast, incubation with low m$\beta$CD:cholesterol ratios increases the cholesterol content of the cells.[41,42] We therefore incubated murine macrophage-like cells with 2.5 mM m$\beta$CD alone or with mixtures of 2.5 mM m$\beta$CD and cholesterol at ratios ranging from 20:1 to 3:1 to decrease and increase the normal levels of cholesterol in the plasma membrane (Figure


dx.doi.org/10.1021/bi3003132 | *Biochemistry* 2012, 51, 3373−3382

5). Binding of $_F$PFO$^{Alexa488}$ was not observed in cells treated with mβCD alone (as in Figure 4B) or with a mβCD:cholesterol ratio of 20:1 (Figure 5). Cells treated with a mβCD:cholesterol ratio of 15:1 were labeled faintly (slightly less than untreated cells) by $_F$PFO$^{Alexa488}$. In contrast, treatment of cells with mβCD:cholesterol ratios of ≤8:1 resulted in substantially more labeling with $_F$PFO$^{Alexa488}$.

The $_F$PFO$^{D434S\ Alexa633}$ derivative was bound to the plasma membrane even when cells were treated with mβCD alone, suggesting that the cholesterol-dependent properties of PFO derivatives observed with model membranes are conserved on natural membranes (i.e., murine macrophage-like cells). A slight increase in the level of binding was observed when cells were treated with a mβCD:cholesterol ratio of 20:1, and a >2-fold increase when cells were treated with ratios of ≤15:1. Interestingly, untreated cells did not significantly bind the $_F$PFO$^{L491S\ Alexa633}$ derivative, suggesting that the cholesterol activity (or availability) in these cells is lower than that obtained in model membranes with 50 mol % cholesterol. Binding of this derivative was observed only on cells overloaded with cholesterol using the lowest mβCD:cholesterol ratios (Figure 5). Taken together, our data clearly indicate that engineered PFO derivatives (e.g., $_F$PFO) could be tuned to associate with cellular membranes containing different cholesterol levels.

## DISCUSSION

Our studies of the role of the membrane-interacting domain of PFO showed that mutations in amino acids located in the proximity of the conserved Cys459 modulated the threshold of cholesterol required to trigger toxin−membrane association. Cholesterol was required at the plasma membrane for binding of PFO to murine macrophage-like cells as determined by both filipin inhibition and cholesterol depletion using mβCD. The differential cholesterol-dependent properties among PFO derivatives were consistent on model as well as natural membranes, and not significantly affected by the lipid composition. Mutations of conserved residues raised or lowered the cholesterol threshold for PFO binding, suggesting that PFO has evolved to recognize an optimal cholesterol chemical activity on cell membranes.

It is widely known that high levels of cholesterol are required in model membranes to trigger binding of PFO and other related CDCs.[22,23,47,48] Similar high-cholesterol-dependent effects have been observed for the enzymatic activity of cholesterol-modifying enzymes (e.g., cholesterol oxidase)[49,50] and for the rate of removal of sterols from the membrane surface by cyclodextrins.[51,52] The high cholesterol levels needed for these membrane processes have been related to the tight interaction of cholesterol molecules with the surrounding phospholipids.[53,54] Cholesterol becomes accessible at the membrane surface only after the sterol−phospholipid interaction is saturated.[4,55] These interactions make the phospholipid/sterol mixtures in membranes nonideal, and therefore, the thermodynamic parameter that more precisely relates to the cholesterol concentration with the accessibility of sterol molecules at the membrane surface is chemical activity. Cholesterol chemical activity (or accessibility) is influenced by changes in the length and saturation of the acyl chains of the phospholipids present in the membrane, as well as by the size of the phospholipid headgroups.[56] Given that the levels of cholesterol on the plasma membrane seem to be tightly regulated,[1,2] it is not unexpected that PFO has evolved to maximize the recognition of a particular cholesterol chemical activity.[20]

PFO contacts the target membrane via D4,[23] the loops at the bottom of the β-sandwich being the only segments of this domain that remain inserted in the membrane after oligomerization (Figure 1).[35] Comparison of the sequences for 28 CDC family members shows that the conserved undecapeptide (residues 458−468, PFO sequence), L1 (residues 488−493), and L2 (residues 398−406) contain five, four, and four invariable residues, respectively.[20] The less conserved L3 (residues 434−439) has no invariable residues. Multiple mutagenesis studies have shown that residues located in the undecapeptide, especially the conserved Trp residues, are very important for pore formation (reviewed in ref 57), and this undecapeptide was initially considered the cholesterol binding site of the CDCs. However, it has been shown that loops L1−L3 are responsible for the interaction of PFO with cholesterol-containing membranes.[32] More recently, it has been suggested that only two invariable residues located in L1 are essential for cholesterol recognition: Thr490 and Leu491.[31] While it is clear that the side chains of T490 and L491 are critical for cholesterol binding, direct cholesterol interaction with these two residues has not been shown. It may be possible that these two mutations affected a membrane-dependent conformational transition required for cholesterol interaction, and not the interaction with cholesterol itself. Moreover, an analysis of other invariable residues located in L1 (Gly488 and Pro493) and L2 (H398, G400, and A404) has not been conducted, and therefore, the exact location of a cholesterol binding site (if any) deserves further characterization. We have shown here the mutation of L491 (a putative cholesterol binding residue) or V403 (not previously related to cholesterol interaction) significantly altered the cholesterol threshold for PFO binding. Surprisingly, none of these residues affected PFO binding or pore formation at high cholesterol concentrations (Figure 2). A similar effect was previously found for the C459A mutation in the undecapeptide (Figure 2A).[28] Moreover, elimination of the negative charge of Asp434 located in the poorly conserved L3 segment lowered the cholesterol threshold for PFO (Figure 3B). It is therefore clear that the nature of amino acids located in D4 loops modulates the cholesterol chemical activity required to trigger toxin binding, with residues located around the conserved Cys459 being the ones that affected the cholesterol threshold the most (Figure 1B). In addition to single-amino acid substitutions, changes that are likely to affect the conformation of the protein, like the pH of the medium, also alter the cholesterol threshold for toxin binding.[26,58] Taken together, these data strongly suggest that the conformation of the PFO D4 dictates the cholesterol chemical activity required to trigger toxin binding. The importance of sensing an optimal cholesterol chemical activity is reflected in the highly conserved amino acid sequences at the membrane interacting loops of the CDCs.

Another important characteristic of binding of PFO to cholesterol-containing membranes is the typical stepwise increase that in our experiments was detected by the intrinsic Trp fluorescence change that follows the exposure of the aromatic residues to the membrane surface.[23,26,29,59] This membrane-dependent fluorescence change constitutes an efficient approach to assessing PFO binding (Figure 3A). The association of PFO with membranes can also be detected by the formation of SDS-resistant oligomers using sodium dodecyl sulfate−polyacrylamide gel electrophoresis.[26,29,60,61] Both ap-


dx.doi.org/10.1021/bi3003132 | Biochemistry 2012, 51, 3373−3382

proaches have independently shown PFO undergo a transition from no binding to complete binding in a very narrow window of cholesterol concentrations. In agreement with these results, we have shown, using simultaneous determinations of PFO binding and pore formation, that the cholesterol-dependent response is regulated during the initial binding step of the toxin.[28] The molecular basis for this sharp cooperative cholesterol-dependent PFO binding remains unknown. It has been suggested that either a sharp change in the cholesterol chemical activity or oligomerization preceded by a reversible PFO−cholesterol equilibrium may be responsible for the sharp change in the binding profile.[29] Similar binding profiles have been observed on membranes containing different levels of cholesterol (e.g., plasma membrane or ER membranes), indicating that similar cholesterol activities can be obtained on membranes with very different cholesterol concentrations.[29] Independent of the mechanism, the effect on the cholesterol threshold for PFO binding observed when the phospholipid composition is modified indicates that cholesterol activity plays a critical role in the initial PFO−membrane interaction.[26−28] This cholesterol-dependent transition has been used to image membranes containing high levels of cholesterol.[62−64] Originally, it was suggested that PFO binds exclusively to cholesterol rich domains or membrane rafts.[19,24] However, it has become clear that PFO binding and membrane localization are not limited to the presence of a particular membrane domain.[26−28,30,65] Therefore, we reasoned that by combining the sharp on−off membrane association properties of PFO with the ability to alter the cholesterol binding threshold of the toxin would provide unique tools for studying and clarifying the cholesterol-dependent binding of PFO to cellular membranes.

Using site-directed mutagenesis, we modified D4 of $_{F}$PFO and obtained two derivatives, $_{F}$PFO$^{D434S}$ and $_{F}$PFO$^{L491S}$, each showing a distinctive cholesterol-dependent profile on model membranes. Binding of $_{F}$PFO$^{D434S}$ required ∼3 mol % less cholesterol than binding of $_{F}$PFO, while binding of $_{F}$PFO$^{L491S}$ required ∼7 mol % more cholesterol than binding of the parental $_{F}$PFO derivative (Figure 3B). On the basis of the cholesterol-dependent response obtained for $_{F}$PFO on murine macrophage-like cells (Figure 4), we determined if the differential binding properties of the proteins were conserved when using cellular membranes. In contrast to the case for model membranes, the distribution and availability of cholesterol on cellular membranes could be affected by many factors, including membrane traffic, synthesis and modifications of lipids, the presence of membrane proteins, and/or the association of the membrane with the cytoskeleton.[66,67] The availability of cholesterol (i.e., cholesterol chemical activity) on the plasma membrane of these cells was varied using incubations with m$\beta$CD alone or different m$\beta$CD/cholesterol mixtures.[41] The level of m$\beta$CD was kept constant at 2.5 mM in all assays to account for any nonspecific effect that this compound may have on membranes (e.g., removal of other lipids). Interestingly, similar cholesterol-dependent properties were observed for PFO derivatives on biological membranes. Only $_{F}$PFO and $_{F}$PFO$^{D434S}$ interacted with untreated murine macrophage-like cells (Figure 5). No significant binding of $_{F}$PFO$^{L491S}$ was detected on murine macrophage-like cells unless the cells were treated with the lowest m$\beta$CD:cholesterol ratios (i.e., the highest cholesterol levels achieved with this procedure). In contrast, $_{F}$PFO$^{D434S}$ was bound to cells treated with m$\beta$CD alone (i.e., the lowest cholesterol level achieved). On the basis of the brighter spots observed along some faint outlines of the plasma membrane, we can speculate that there is heterogeneity in the distribution of cholesterol in the plasma membrane. As observed with model membranes, the binding properties of the parental $_{F}$PFO derivative on murine macrophage-like cell membranes were intermediate when compared with the properties observed for $_{F}$PFO$^{D434S}$ and $_{F}$PFO$^{L491S}$ (Figure 5).

In summary, we have shown here that modifications on PFO D4 altered the cholesterol binding properties of the toxin. Moreover, engineered PFO derivatives differentially bind to model and biological membranes containing different cholesterol levels. The plasticity of the PFO−cholesterol interaction combined with engineered PFO derivatives will allow us and others to create novel molecular probes for studying the cholesterol distribution and dynamics on cellular membranes.

## ■ ASSOCIATED CONTENT

### Supporting Information

Oligomerization of FPFO as determined by BODIPY self-quenching and the hemolytic activity of nPFO, rPFO, and $_{F}$PFO. This material is available free of charge via the Internet at http://pubs.acs.org.

## ■ AUTHOR INFORMATION


### Corresponding Author

*Address: 710 N. Pleasant St., Lederle GRT, Rm 816, University of Massachusetts, Amherst, MA 01003. Phone: (413) 545-2497. Fax: (413) 545-3291. E-mail: heuck@biochem.umass.edu.



### Funding

This research was supported in part by a Scientist Development Grant (0830136N) from the American Heart Association to A.P.H. and a grant (MOP 74753) from the Canadian Institutes of Health Research to B.L.T.

### Notes

The authors declare no competing financial interest.


## ■ ACKNOWLEDGMENTS


We thank Kathryne Medeiros for the creation and initial characterization of the $_{F}$PFO$^{D434S}$ derivative.


## ■ ABBREVIATIONS

PFO, perfringolysin O; CDC, cholesterol-dependent cytolysin; LDL, low-density lipoprotein; DX, domain *X* (*X* = 1, 2, 3, or 4); nPFO, native PFO; rPFO, nPFO$^{C459A}$, where the superscript indicates that the derivative has C459 substituted with an alanine; $_{F}$PFO, rPFO$^{E167C/F318A}$; POPC, 1-palmitoyl-2-oleoyl-*sn*-glycero-3-phosphocholine; POPE, 1-palmitoyl-2-oleoyl-*sn*-glycero-3-phosphoethanolamine; SM, sphingomyelin; m$\beta$CD, methyl-$\beta$-cyclodextrin; DAPI, 4′,6-diamidino-2-phenylindole; CTxB, cholera toxin subunit B; LX, loop *X* (*X* = 1, 2, or 3).

## ■ REFERENCES


(1) Steck, T. L., and Lange, Y. (2010) Cell cholesterol homeostasis: Mediation by active cholesterol. *Trends Cell Biol. 20*, 680−687.

(2) Maxfield, F. R., and van Meer, G. (2010) Cholesterol, the central lipid of mammalian cells. *Curr. Opin. Cell Biol. 22*, 422−429.

(3) Ikonen, E. (2008) Cellular cholesterol trafficking and compartmentalization. *Nat. Rev. Mol. Cell Biol. 9*, 125−138.

(4) Mesmin, B., and Maxfield, F. R. (2009) Intracellular sterol dynamics. *Biochim. Biophys. Acta 1791*, 636−645.

(5) Maxfield, F. R., and Tabas, I. (2005) Role of cholesterol and lipid organization in disease. *Nature 438*, 612−621.
(6) Vainio, S., and Ikonen, E. (2003) Macrophage cholesterol transport: A critical player in foam cell formation. *Ann. Med. 35*, 146−155.
(7) Tabas, I. (2005) Consequences and therapeutic implications of macrophage apoptosis in atherosclerosis: The importance of lesion stage and phagocytic efficiency. *Arterioscler. Thromb. Vasc. Biol. 25*, 2255−2264.
(8) Blanchette-Mackie, E. J. (2000) Intracellular cholesterol trafficking: Role of the NPC1 protein. *Biochim. Biophys. Acta 1486*, 171−183.
(9) Ikonen, E., and Holtta-Vuori, M. (2004) Cellular pathology of Niemann-Pick type C disease. *Semin. Cell Dev. Biol. 15*, 445−454.
(10) Puglielli, L., Tanzi, R. E., and Kovacs, D. M. (2003) Alzheimer's disease: The cholesterol connection. *Nat. Neurosci. 6*, 345−351.
(11) Neufeld, E. B., Cooney, A. M., Pitha, J., Dawidowicz, E. A., Dwyer, N. K., Pentchev, P. G., and Blanchette-Mackie, E. J. (1996) Intracellular trafficking of cholesterol monitored with a cyclodextrin. *J. Biol. Chem. 271*, 21604−21613.
(12) Wustner, D., Mondal, M., Tabas, I., and Maxfield, F. R. (2005) Direct observation of rapid internalization and intracellular transport of sterol by macrophage foam cells. *Traffic 6*, 396−412.
(13) Rust, M. J., Bates, M., and Zhuang, X. (2006) Sub-diffraction-limit imaging by stochastic optical reconstruction microscopy (STORM). *Nat. Methods 3*, 793−795.
(14) Willig, K. I., Kellner, R. R., Medda, R., Hein, B., Jakobs, S., and Hell, S. W. (2006) Nanoscale resolution in GFP-based microscopy. *Nat. Methods 3*, 721−723.
(15) Giepmans, B. N. G., Adams, S. R., Ellisman, M. H., and Tsien, R. Y. (2006) The fluorescent toolbox for assessing protein location and function. *Science 312*, 217−224.
(16) Wustner, D. (2007) Fluorescent sterols as tools in membrane biophysics and cell biology. *Chem. Phys. Lipids 146*, 1−25.
(17) Coxey, R. A., Pentchev, P. G., Campbell, G., and Blanchette-Mackie, E. J. (1993) Differential accumulation of cholesterol in Golgi compartments of normal and Niemann-Pick type C fibroblasts incubated with LDL: A cytochemical freeze-fracture study. *J. Lipid Res. 34*, 1165−1176.
(18) Miller, R. G. (1984) The use and abuse of filipin to localize cholesterol in membranes. *Cell Biol. Int. Rep. 8*, 519−535.
(19) Waheed, A., Shimada, Y., Heijnen, H. F. G., Nakamura, M., Inomata, M., Hayashi, M., Iwashita, S., Slot, J. W., and Ohno-Iwashita, Y. (2001) Selective binding of perfringolysin O derivative to cholesterol-rich membrane microdomains (rafts). *Proc. Natl. Acad. Sci. U.S.A. 98*, 4926−4931.
(20) Heuck, A. P., Moe, P. C., and Johnson, B. B. (2010) The cholesterol-dependent cytolysins family of Gram-positive bacterial toxins. In *Cholesterol binding proteins and cholesterol transport* (Harris, J. R., Ed.) pp 551−577, Springer, Berlin.
(21) Robinson, J. M., and Karnovsky, M. J. (1980) Evaluation of the polyene antibiotic filipin as a cytochemical probe for membrane cholesterol. *J. Histochem. Cytochem. 28*, 161−168.
(22) Ohno-Iwashita, Y., Iwamoto, M., Ando, S., and Iwashita, S. (1992) Effect of lipidic factors on membrane cholesterol topology: Mode of binding of $\theta$-toxin to cholesterol in liposomes. *Biochim. Biophys. Acta 1109*, 81−90.
(23) Heuck, A. P., Hotze, E. M., Tweten, R. K., and Johnson, A. E. (2000) Mechanism of membrane insertion of a multimeric $\beta$-barrel protein: Perfringolysin O creates a pore using ordered and coupled conformational changes. *Mol. Cell 6*, 1233−1242.
(24) Ohno-Iwashita, Y., Shimada, Y., Waheed, A., Hayashi, M., Inomata, M., Nakamura, M., Maruya, M., and Iwashita, M. (2004) Perfringolysin O, a cholesterol-binding cytolysin, as a probe for lipid rafts. *Anaerobe, 10*, 125−134.
(25) Ohno-Iwashita, Y., Shimada, Y., Hayashi, M., Iwamoto, M., Iwashita, S., and Inomata, M. (2010) Cholesterol-binding toxins and anti-cholesterol antibodies as structural probes for cholesterol localization. In *Cholesterol Binding and Cholesterol Transport Proteins* (Harris, J. R., Ed.) pp 597−621, Springer, Berlin.
(26) Nelson, L. D., Johnson, A. E., and London, E. (2008) How interaction of perfringolysin O with membranes is controlled by sterol structure, lipid structure, and physiological low pH: Insights into the origin of perfringolysin O-lipid raft interaction. *J. Biol. Chem. 283*, 4632−4642.
(27) Flanagan, J. J., Tweten, R. K., Johnson, A. E., and Heuck, A. P. (2009) Cholesterol exposure at the membrane surface is necessary and sufficient to trigger perfringolysin O binding. *Biochemistry 48*, 3977−3987.
(28) Moe, P. C., and Heuck, A. P. (2010) Phospholipid hydrolysis caused by *Clostridium perfringens* $\alpha$-toxin facilitates the targeting of perfringolysin O to membrane bilayers. *Biochemistry 49*, 9498−9507.
(29) Sokolov, A., and Radhakrishnan, A. (2010) Accessibility of cholesterol in endoplasmic reticulum membranes and activation of SREBP-2 switch abruptly at a common cholesterol threshold. *J. Biol. Chem. 285*, 29480−29490.
(30) Heuck, A. P., Savva, C. G., Holzenburg, A., and Johnson, A. E. (2007) Conformational changes that effect oligomerization and initiate pore formation are triggered throughout perfringolysin O upon binding to cholesterol. *J. Biol. Chem. 282*, 22629−22637.
(31) Farrand, A. J., LaChapelle, S., Hotze, E. M., Johnson, A. E., and Tweten, R. K. (2010) Only two amino acids are essential for cytolytic toxin recognition of cholesterol at the membrane surface. *Proc. Natl. Acad. Sci. U.S.A. 107*, 4341−4346.
(32) Soltani, C. E., Hotze, E. M., Johnson, A. E., and Tweten, R. K. (2007) Structural elements of the cholesterol-dependent cytolysins that are responsible for their cholesterol-sensitive membrane interactions. *Proc. Natl. Acad. Sci. U.S.A. 104*, 20226−20231.
(33) Ramachandran, R., Tweten, R. K., and Johnson, A. E. (2004) Membrane-dependent conformational changes initiate cholesterol-dependent cytolysin oligomerization and intersubunit $\beta$-strand alignment. *Nat. Struct. Mol. Biol. 11*, 697−705.
(34) Ramachandran, R., Tweten, R. K., and Johnson, A. E. (2005) The domains of a cholesterol-dependent cytolysin undergo a major FRET-detected rearrangement during pore formation. *Proc. Natl. Acad. Sci. U.S.A. 102*, 7139−7144.
(35) Ramachandran, R., Heuck, A. P., Tweten, R. K., and Johnson, A. E. (2002) Structural insights into the membrane-anchoring mechanism of a cholesterol-dependent cytolysin. *Nat. Struct. Mol. Biol. 9*, 823−827.
(36) Shepard, L. A., Heuck, A. P., Hamman, B. D., Rossjohn, J., Parker, M. W., Ryan, K. R., Johnson, A. E., and Tweten, R. K. (1998) Identification of a membrane-spanning domain of the thiol-activated pore-forming toxin *Clostridium perfringens* perfringolysin O: An $\alpha$-helical to $\beta$-sheet transition identified by fluorescence spectroscopy. *Biochemistry 37*, 14563−14574.
(37) Solovyova, A. S., Nollmann, M., Mitchell, T. J., and Byron, O. (2004) The solution structure and oligomerization behavior of two bacterial toxins: Pneumolysin and perfringolysin O. *Biophys. J. 87*, 540−552.
(38) Romano, F. B., Rossi, K. C., Savva, C. G., Holzenburg, A., Clerico, E. M., and Heuck, A. P. (2011) Efficient isolation of *Pseudomonas aeruginosa* type III secretion translocators and assembly of heteromeric transmembrane pores in model membranes. *Biochemistry 50*, 7117−7131.
(39) Heuck, A. P., Tweten, R. K., and Johnson, A. E. (2003) Assembly and topography of the prepore complex in cholesterol-dependent cytolysins. *J. Biol. Chem. 278*, 31218−31225.
(40) Chen, P. S., Toribara, T. Y., and Warner, H. (1956) Microdetermination of phosphorus. *Anal. Chem. 28*, 1756−1758.
(41) Christian, A. E., Haynes, M. P., Phillips, M. C., and Rothblat, G. H. (1997) Use of cyclodextrins for manipulating cellular cholesterol content. *J. Lipid Res. 38*, 2264−2272.
(42) Gimpl, G., Burger, K., and Fahrenholz, F. (1997) Cholesterol as modulator of receptor function. *Biochemistry 36*, 10959−10974.
(43) Pang, L., Graziano, M., and Wang, S. (1999) Membrane cholesterol modulates galanin-GalR2 interaction. *Biochemistry 38*, 12003−12011.

(44) Gimpl, G., and Gehrig-Burger, K. (2011) Probes for studying cholesterol binding and cell biology. *Steroids 76*, 216−231.
(45) Wolf, A. A., Fujinaga, Y., and Lencer, W. I. (2002) Uncoupling of the cholera toxin-GM1 ganglioside receptor complex from endocytosis, retrograde Golgi trafficking, and downstream signal transduction by depletion of membrane cholesterol. *J. Biol. Chem. 277*, 16249−16256.
(46) Zidovetzki, R., and Levitan, I. (2007) Use of cyclodextrins to manipulate plasma membrane cholesterol content: Evidence, misconceptions and control strategies. *Biochim. Biophys. Acta 1768*, 1311−1324.
(47) Alving, C. R., Habig, W. H., Urban, K. A., and Hardegree, M. C. (1979) Cholesterol-dependent tetanolysin damage to liposomes. *Biochim. Biophys. Acta 551*, 224−228.
(48) Rosenqvist, E., Michaelsen, T. E., and Vistnes, A. I. (1980) Effect of streptolysin O and digitonin on egg lecithin/cholesterol vesicles. *Biochim. Biophys. Acta 600*, 91−102.
(49) Patzer, E. J., and Wagner, R. R. (1978) Cholesterol oxidase as a probe for studying membrane organisation. *Nature 274*, 394−395.
(50) Lange, Y., Cutler, H. B., and Steck, T. L. (1980) The effect of cholesterol and other intercalated amphipaths on the contour and stability of the isolated red cell membrane. *J. Biol. Chem. 255*, 9331−9337.
(51) Radhakrishnan, A., and McConnell, H. M. (2000) Chemical activity of cholesterol in membranes. *Biochemistry 39*, 8119−8124.
(52) Leventis, R., and Silvius, J. R. (2001) Use of cyclodextrins to monitor transbilayer movement and differential lipid affinities of cholesterol. *Biophys. J. 81*, 2257−2267.
(53) Huang, J., and Feigenson, G. W. (1999) A microscopic interaction model of maximum solubility of cholesterol in lipid bilayers. *Biophys. J. 76*, 2142−2157.
(54) McConnell, H. M., and Radhakrishnan, A. (2003) Condensed complexes of cholesterol and phospholipids. *Biochim. Biophys. Acta 1610*, 159−173.
(55) Lange, Y., Ye, J., and Steck, T. L. (2004) How cholesterol homeostasis is regulated by plasma membrane cholesterol in excess of phospholipids. *Proc. Natl. Acad. Sci. U.S.A. 101*, 11664−11667.
(56) Ohvo-Rekilä, H., Ramstedt, B., Leppimäki, P., and Slotte, J. P. (2002) Cholesterol interactions with phospholipids in membranes. *Prog. Lipid Res. 41*, 66−97.
(57) Alouf, J. E., Billington, S. J., and Jost, B. H. (2006) Repertoire and general features of the family of cholesterol-dependent cytolysins. In *The Comprehensive Sourcebook of Bacterial Protein Toxins* (Alouf, J. E., and Popoff, M. R., Eds.) pp 643−658, Academic Press, Oxford, England.
(58) Bavdek, A., Gekara, N. O., Priselac, D., Gutierrez Aguirre, I., Darji, A., Chakraborty, T., Maček, P., Lakey, J. H., Weiss, S., and Anderluh, G. (2007) Sterol and pH interdependence in the binding, oligomerization, and pore formation of listeriolysin O. *Biochemistry 46*, 4425−4437.
(59) Sekino-Suzuki, N., Nakamura, M., Mitsui, K.-I., and Ohno-Iwashita, Y. (1996) Contribution of individual tryptophan residues to the structure and activity of $\theta$-toxin (perfringolysin O), a cholesterol-binding cytolysin. *Eur. J. Biochem. 241*, 941−947.
(60) Shepard, L. A., Shatursky, O., Johnson, A. E., and Tweten, R. K. (2000) The mechanism of pore assembly for a cholesterol-dependent cytolysin: Formation of a large prepore complex precedes the insertion of the transmembrane $\beta$-hairpins. *Biochemistry 39*, 10284−10293.
(61) Hotze, E. M., Wilson-Kubalek, E. M., Rossjohn, J., Parker, M. W., Johnson, A. E., and Tweten, R. K. (2001) Arresting pore formation of a cholesterol-dependent cytolysin by disulfide trapping synchronizes the insertion of the transmembrane $\beta$-sheet from a prepore intermediate. *J. Biol. Chem. 276*, 8261−8268.
(62) Reid, P. C., Sakashita, N., Sugii, S., Ohno-Iwashita, Y., Shimada, Y., Hickey, W. F., and Chang, T.-Y. (2004) A novel cholesterol stain reveals early neuronal cholesterol accumulation in the Niemann-Pick type C1 mouse brain. *J. Lipid Res. 45*, 582−591.
(63) Hayashi, M., Shimada, Y., Inomata, M., and Ohno-Iwashita, Y. (2006) Detection of cholesterol-rich microdomains in the inner leaflet of the plasma membrane. *Biochem. Biophys. Res. Commun. 351*, 713−718.
(64) Koseki, M., Hirano, K.-i., Masuda, D., Ikegami, C., Tanaka, M., Ota, A., Sandoval, J. C., Nakagawa-Toyama, Y., Sato, S. B., Kobayashi, T., Shimada, Y., Ohno-Iwashita, Y., Matsuura, F., Shimomura, I., and Yamashita, S. (2007) Increased lipid rafts and accelerated lipopolysaccharide-induced tumor necrosis factor-$\alpha$ secretion in Abca1-deficient macrophages. *J. Lipid Res. 48*, 299−306.
(65) Nelson, L. D., Chiantia, S., and London, E. (2010) Perfringolysin O association with ordered lipid domains: Implications for transmembrane protein raft affinity. *Biophys. J. 99*, 3255−3263.
(66) Silvius, J. (2005) Lipid microdomains in model and biological membranes: How strong are the connections? *Q. Rev. Biophys. 38*, 373−383.
(67) Gaus, K., Rodriguez, M., Ruberu, K. R., Gelissen, I., Sloane, T. M., Kritharides, L., and Jessup, W. (2005) Domain-specific lipid distribution in macrophage plasma membranes. *J. Lipid Res. 46*, 1526−1538.